MODEL SELECTION FOR ENERGY DISSIPATION MECHANISMS

Stipe PERIŠIĆ[1], Jani BARLE[2], Nikola SOKOL[3], Predrag ĐUKIĆ[4]

[1] 0000-0001-5825-1193, FESB, Ulica Ruđera Boškovića 32, Split, Croatia, E-mail: sperisic@fesb.hr;

[2] 0000-0002-5861-2240, FESB, Ulica Ruđera Boškovića 32, Split, Croatia, E-mail: jbarle@fesb.hr;

[3] FESB, Ulica Ruđera Boškovića 32, Split, Croatia, E-mail: Nikola.Sokol.00@fesb.hr

[4] 0000-0002-6057-3201, DPS, Kopilica 5, 21000 Split, Croatia E-mail: pdukic@oss.unist.hr

1. Introduction

In order to perform efficient and robust system analysis, linear models are frequently used. While this approach is often justified in practice, certain scenarios require the use of more complex models [1]. Therefore, the focus of this paper is on selecting the optimal model based on the collected data using the Akaike Information Criterion (AIC) [2]. The criterion is demonstrated on energy dissipation models related to dynamic systems. Although a wide range of models exists, the most commonly used are the viscous model, the Coulomb friction model, and a combination of the two. As a proof of concept, two energy dissipation models, the standalone Coulomb friction model [3] and a combined viscous-Coulomb model [4] are analyzed using free decay oscillation signals. The analysis is conducted via envelope fitting to ensure a fast and efficient model selection process.

2. AIC and Dynamic model used

The AIC belongs to the class of log-predictive densities and is developed under the assumption that models are estimated via maximum likelihood. It is expressed by Eq. (1):

$$AIC = 2c - 2ln(L) \tag{1}$$

where c is number of model parameters and L is model likelihood. The model with lowest AIC value is considered as better fit.

$$m\ddot{x} + F\ + kx = f(t) \tag{2}$$

To determine the optimal energy dissipation model for the second-order system described by Eq. (2), two models were evaluated: Coulomb friction, and a combination of viscous damping and Coulomb model defined in Eq. (3) and (4), respectively.

$$F = r\ sign(\dot{x}) \tag{3}$$

$$F = d\dot{x} + r\ sign(\dot{x}) \tag{4}$$

Parameters d and r are viscous damping coefficient and Coulomb dry friction force. To test the model selection, a numerical example was first considered. The target system was a second-order model (Eq. 2) incorporating both viscous damping and Coulomb friction (Eq. 5) as the energy dissipation mechanisms. Parameters were set to m=10 kg and k = 3000 N/m, with r = 0.15 N and d = 3 Ns/m. Also normal distribution was added to response with $\sigma = 5 \cdot 10^{-4}$ to simulate operating conditions.

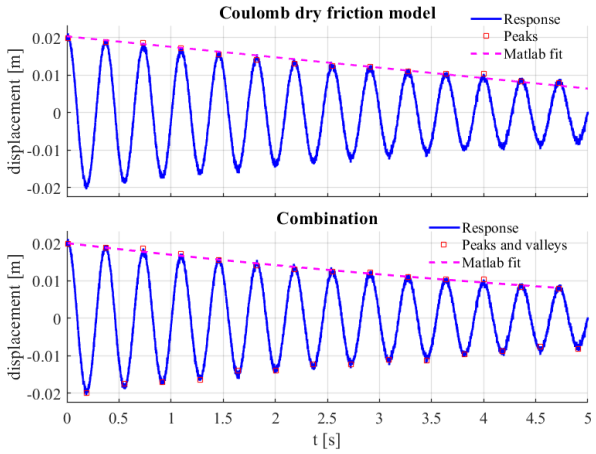


Fig. 1. Simulate response and fitted envelope

The simulated responses and fitted envelopes are presented in Fig. 1. Envelope fitting is carried out with the MATLAB® built-in function *fit* with nonlinear least squares method. A visual inspection suggests that both models appear adequate. However, applying the AIC selection process (Table 1) identifies the Friction model as the most suitable. Additionally, Table 1 includes model selection based on the RMSE. According to the RMS error, the combined model is the best option, which corresponds to the true model.

In general, the AIC penalizes models with more parameters. In this case, it identifies the Coulumb model as optimal because the noisy data does not justify the usage of a more complex model. In

contrast, the RMSE criterion tends to favor more complex models.

Table 1. Model selection via AIC and RMSE

Model	AIC	RMSE
Coulomb	-160.1	0.00070
Combination	-168.1	0.00046

In the second case, the model parameters remained identical except for the noise level, which was reduced to $\sigma = 2 \cdot 10^{-4}$. While the graphical representation of these results is omitted for brevity reasons, the AIC now supports a more complex model due to the increased signal-to-noise ratio. This justifies the application of the AIC to experimental signals, as demonstrated in the next section.

3. Experimental model and discussion

The experimental setup shown in Fig. 2 is a SDoF rolling bearing system with $m = 7.654$ kg and $k = 5835$ N/m wile damping model and its value is unknown. Displacement was measured via a Honeywell SPS-L225-HALS sensor and acquired using an NI-USB-6251 at 1 kHz.

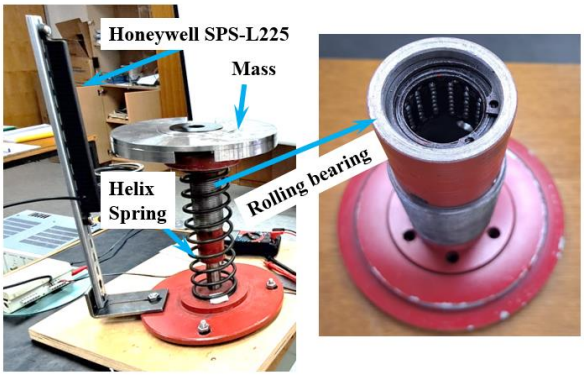


Fig. 2. Experimental test bed

The test bed motion was induced by an initial displacement of 9 mm. Here, two models, Coulomb, and their combination of viscous and Coulomb model were fitted to the response also. The result of envelope fitting can be seen in Fig. 3.

Table 2. Model selection via AIC and RMSE

Model	AIC	RMSE
Coulomb	-79.2679	0.00021721
Combination	-63.5079	0.00036862

Table 2 presents the model selection results. According to the AIC, the Coulomb model is the optimal choice here, which is expected given the mechanical contact involved and the limited data set. This is further supported by the RMSE, although the Coulomb model only marginally outperforms the combined model. In contrast, the AIC values show a significant preference for the standalone Coulomb model.

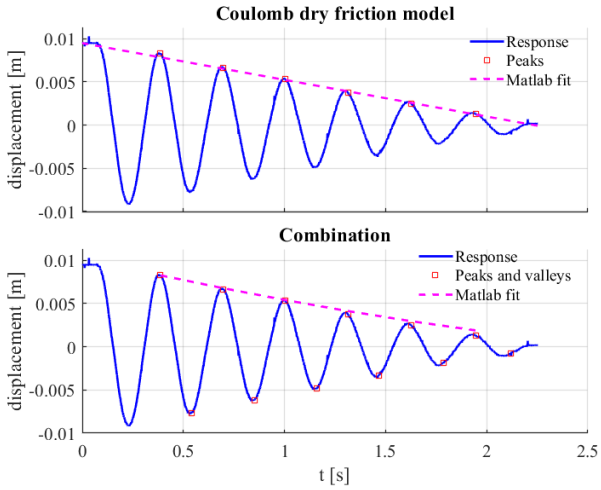


Fig. 2 Fitted envelopes for 9 mm initial displacement

4. Conclusions

As demonstrated, the AIC provides a simple and effective approach for selecting the optimal energy dissipation model. By balancing accuracy and complexity, it reduces selection errors compared to the standard RMSE. Furthermore, efficiency is boosted by fitting signal envelopes rather than full waveforms. This combination of speed and reliability makes the approach highly suitable for practical engineering analysis.

Acknowledgments

This work was supported by the EU under the NextGenerationEU instrument, through the Recovery and Resilience Mechanism, within the institutional research project AIMTECH 4.5 (IP-UNIST-07), implemented by the Ministry of Science, Education and Youth of the Republic of Croatia.

References

[1] Salgueiro J, Peršin G, Vižintin J, Ivanovič M, Dolenc B. On-line Oil Monitoring and Diagnosis. *Strojniški Vestn – J Mech Eng* 2013;10:604–12. https://doi.org/10.5545/sv-jme.2013.973.

[2] Ding J, Tarokh V, Yang Y. Model selection techniques – an overview. IEEE Signal Process 2018;35:16–34. https://doi.org/10.1109/MSP.2018.2867638.

[3] Hanaor DAH, Gan Y, Einav I. Static friction at fractal interfaces. Tribol Int 2016;93:229–38. https://doi.org/10.1016/j.triboint.2015.09.016.

[4] Liang, J.W., Feeny BF. Identifying Coulomb and Viscous Friction from Free-Vibration Decrements. Nonlinear Dyn 1998:337–47. https://doi.org/10.1023/A:1008213814102.